Research Article

Journal of Innate Immunity

J Innate Immun 2015;7:612–622
DOI: 10.1159/000430498

Received: September 4, 2014
Accepted after revision: April 15, 2015
Published online: May 14, 2015

Group A *Streptococcus* Modulates Host Inflammation by Manipulating Polymorphonuclear Leukocyte Cell Death Responses

James A. Tsatsaronis[a] Diane Ly[a] Aleta Pupovac[a] Oliver Goldmann[c] Manfred Rohde[d] Jude M. Taylor[a] Mark J. Walker[b] Eva Medina[c] Martina L. Sanderson-Smith[a]

[a]Illawarra Health and Medical Research Institute and School of Biological Sciences, University of Wollongong, Wollongong, N.S.W., and [b]Australian Infectious Diseases Research Centre and School of Chemistry and Molecular Biosciences, University of Queensland, St. Lucia, Qld., Australia; [c]Infection Immunology Research Group and [d]Central Facility for Microscopy, Helmholtz Centre for Infection Research, Braunschweig, Germany

Key Words
Neutrophils · Apoptosis · Oncosis · *Streptococcus pyogenes*

Abstract
Polymorphonuclear leukocyte (PMN) cell death strongly influences the resolution of inflammatory episodes, and may exacerbate adverse pathologies in response to infection. We investigated PMN cell death mechanisms following infection by virulent group A *Streptococcus* (GAS). Human PMNs were infected in vitro with a clinical, virulent GAS isolate and an avirulent derivative strain, and compared for phagocytosis, the production of reactive oxygen species (ROS), mitochondrial membrane depolarization and apoptotic markers. C57BL/6J mice were then infected, in order to observe the effects on murine PMNs in vivo. Human PMNs phagocytosed virulent GAS less efficiently, produced less ROS and underwent reduced mitochondrial membrane depolarization compared with phagocytosis of avirulent GAS. Morphological and biochemical analyses revealed that PMNs infected with avirulent GAS exhibited nuclear fragmentation and caspase-3 activation consistent with an anti-inflammatory apoptotic phenotype. Conversely, virulent GAS induced PMN vacuolization and plasma membrane permeabilization, leading to a necrotic form of cell death. Infection of the mice with virulent GAS engendered significantly higher systemic pro-inflammatory cytokine release and localized infiltration of murine PMNs, with cells associated with virulent GAS infection exhibiting reduced apoptotic potential. Avirulent GAS infection was associated with lower levels of proinflammatory cytokines and tissue PMN apoptosis. We propose that the differences in PMN cell death mechanisms influence the inflammatory responses to infection by GAS.

Introduction

Programmed cell death determines the fate of circulating polymorphonuclear leukocytes (PMNs) and those recruited to sites of infection. PMNs are rapidly and spontaneously apoptotic under physiological conditions, a phenotype also prominent during bacterial infection [1]. After phagocytosis, senescent PMNs initiate an apoptotic program that shuts down cellular processes and blunts inflammatory potential [2, 3]. The initiation of phagocytosis-induced cell death triggers the expression of 'eat-me' signals on these cells and marks them for

1662–811X/15/0076–0612$39.50/0

E-Mail karger@karger.com
www.karger.com/jin

Dr. Martina L. Sanderson-Smith
Illawarra Health and Medical Research Institute (IHMRI), School of Biological Sciences
University of Wollongong, Northfields Avenue
Wollongong, NSW 2522 (Australia)
E-Mail martina@uow.edu.au

phagocytosis by tissue-resident and recruited macrophages; this is called efferocytosis [4]. Macrophage efferocytosis of apoptotic PMNs reduces the accidental release of stored PMN granules, and thus prevents the potential for PMN-mediated collateral damage to the surrounding tissues [5]. However, numerous pathogens have been shown to be capable of prompting alternative leukocyte cell death mechanisms, including pyroptosis and oncosis [6, 7]. Whilst the induction of PMN apoptosis and efferocytosis imparts a strong anti-inflammatory action on the surrounding tissues, pathogenic stimulation of pyroptosis and oncosis prompt pro-inflammatory cell phenotypes that lead to eventual cell death. Thus, dysregulation of native PMN apoptosis may stimulate gratuitous inflammatory responses via the uncontrolled release of granular contents and other pro-inflammatory cytosolic factors [8].

Group A *Streptococcus* (*Streptococcus pyogenes*; GAS) is the etiological agent of severe diseases with inflammatory involvement, including necrotizing fasciitis (NF) and septic shock [9, 10]. Epidemiologically, GAS disease accounts for >663,000 cases of invasive infections globally [11]. Almost a third of NF cases lead to mortality in developed countries, a fraction that rises to 50% in cases with associated toxic shock [12]. Severe inflammation and destruction of focal tissues is a hallmark of NF infection. Furthermore, GAS sepsis is accompanied by the systemic release of numerous pro-inflammatory mediators, with the magnitude of inflammatory cytokine response strongly correlated to the severity of the disease [13]. GAS alteration of PMN cell death may therefore strongly influence clinical manifestations of inflammatory GAS disease. Here, we examine the potential of virulent and avirulent GAS strains to modulate PMN cell death responses as well as the associated effect of GAS-induced PMN cell death on inflammatory responses.

Materials and Methods

Ethics Approval

All work involving the use of human blood and blood products was conducted with the informed consent of the volunteers and was approved by the University of Wollongong Human Ethics Committee. All animal use and procedures were approved by the University of Wollongong Animal Ethics Committee.

Bacterial Strains

The clinical GAS bacteremia isolate NS88.2 (*emm*98.1) encoding a nonfunctional control of virulence regulator *(covRS)* and the functional *covRS* derivative NS88.2*rep* strain have been previously described [14]. NS88.2 and NS88.2*rep* strains expressing enhanced green fluorescent protein (eGFP) were constructed via transformation with the pDC-eGFP vector [15]. GAS strains were routinely cultured at 37°C on solid horse-blood agar (Thermo Fisher Scientific, Waltham, Mass., USA) or Todd-Hewitt agar (BD Bioscience, Franklin Lakes, N.J., USA), in static cultures of yeast-supplemented (1% w/v) Todd-Hewitt broth (THY) or in static THY cultures supplemented with 2 μg/ml erythromycin for maintenance of the pDC-eGFP vector.

Isolation of Human PMNs

Human venous blood was taken into citrated polypropylene tubes, overlaid onto PolyMorphPrep (Axis-Shield, Oslo, Norway). PMNs were purified as per the manufacturer's instructions and maintained in Roswell-Park Memorial Institute (RPMI) medium containing 2% heat-inactivated plasma. The purity of the human PMN preparations via this method was estimated to be >98%, as exhibited by the characteristic forward- and side-scatter profiles and CD14 staining for contaminating monocytes of PMN samples (online suppl. fig. S1; for all online suppl. material, see www.karger.com/doi/10.1159/000430498).

In vitro Infection of Human PMNs with GAS

GAS cultures were routinely prepared for in vitro human PMN infection via growth to the mid-logarithmic phase, washing twice with sterile PBS and diluted to the required inoculum in RPMI containing 2% heat-inactivated human plasma. Purified human PMNs were seeded into either 96-well (for phagocytosis, cytotoxicity and the production of reactive oxygen species (ROS)) or 24-well plates (for microscopy, TUNEL and Western blot) and GAS was added to the appropriate multiplicity of infection (MOI, PMNs:GAS). PMN phagocytosis was synchronized via centrifugation at 380 *g* for 8 min at 4°C prior to incubation at 37°C in 5% CO_2. In some experiments, PMNs were treated with 5 μg/ml of cytochalasin D (Cayman Chemicals, Ann Arbor, Mich., USA) for 30 min at room temperature prior to infection.

Phagocytosis of GAS

To measure GAS uptake by PMNs, 5×10^5 cells were infected with 5×10^6 CFU of eGFP-expressing GAS and incubated for varying times (5, 40, 80 and 120 min) or for 40 min at varying MOIs (1:5, 1:10, 1:20 and 1:40). The association of GAS with PMNs was measured using an LSR II flow cytometer (BD Bioscience), calculated as the percentage of PMNs with eGFP fluorescence relative to uninfected PMNs. The relative quantity of GAS associated with PMNs was estimated by the mean fluorescence intensity (MFI) of eGFP-positive PMNs. Double immunofluorescence of infected PMNs was conducted by in vitro infection of 1×10^6 PMNs with 1×10^7 GAS on prepared coverslips, with subsequent incubation for 30 min. After incubation, cells were fixed with 4% paraformaldehyde and extracellular GAS was labeled with polyclonal rabbit anti-GAS antiserum and mouse anti-rabbit Alexa Fluor 488-conjugated IgG (Dako, Glostrup, Denmark). Samples were then permeabilized with 0.1% Triton-X for 5 min and extracellular and intracellular GAS were labeled with polyclonal rabbit anti-GAS antiserum and mouse anti-rabbit Alexa Fluor 568-conjugated IgG (Dako). Slides were mounted with Prolong Gold containing DAPI (Invitrogen, Carlsbad, Calif., USA) and then visualized using an Axio Observer inverted microscope (Carl Zeiss, Oberkochen, Germany). Microscope images were altered for brightness and contrast to highlight the infecting GAS cells.

ROS Production

Kinetic measurement of PMN ROS production was conducted essentially as previously [2]. Briefly, purified PMNs were loaded with 25 μM of dichlorofluorescein (DCF, Molecular Probes, Eugene, Oreg., USA) for 40 min in the dark at room temperature, prior to the infection of 5×10^5 PMNs with 5×10^6 GAS CFU. PMN ROS production was measured fluorometrically (λ_{ex}: 488 nm, λ_{emm}: 515 nm) using a POLARstar Omega fluorescent plate reader (BMG Labtech, Carlsbad, Calif., USA).

Estimation of PMN Mitochondrial Membrane Potential

The depolarization of mitochondrial membranes of infected PMNs was estimated using an established technique [6]. Briefly, purified PMNs were loaded with 5 μM of 3,3′-dihexyloxacarbocyanine [$DiOC_6(3)$] iodide for 20 min at room temperature prior to 2 h of GAS infection. Perturbation of the Ψ_m (mitochondrial membrane potential) was indicated as a loss of $DiOC_6(3)$ fluorescence compared to time 0 uninfected PMNs determined by means of a FACSCalibur flow cytometer (BD Bioscience).

Western Blot of Cleaved Caspase-3

Caspase-3 cleavage was detected via Western blotting of cell lysates from infected PMNs. In vitro infections of 2×10^6 PMNs with 2×10^7 GAS CFU were conducted for the time points indicated and cell lysates were run on SDS-PAGE gels prior to transfer to nitrocellulose membranes and probing using mouse anti-caspase-3 IgG (Biolegend, San Diego, Calif., USA), rabbit anti-actin IgG (Sigma-Aldrich, St. Louis, Mo., USA) and detection using HRP-conjugated IgGs (Bio-Rad, Berkely, Calif., USA).

Staining of Purified PMNs

Assessment of apoptosis induced nuclear DNA fragmentation was quantified by terminal deoxynucleotidyl transferase dUTP nick-end labelling (TUNEL) using the DEADend fluorometric TUNEL kit (Promega, Fitchburg, Wis., USA) as per the manufacturer's instructions and an LSR II flow cytometer (BD Bioscience).

Animal Infection Studies

Subcutaneous GAS challenge of C57BL/6J mice has been described previously [14]. Estimation of bacterial survival in vivo and GAS interaction with murine PMNs were conducted by the method of Ly et al. [16], C57BL/6J mice were anesthetized via isoflurane inhalation, and 2×10^7 CFU of mid-logarithmic phase eGFP-expressing GAS were injected intradermally into the left and right flanks prior to incubation for 6 h. The mice were subsequently euthanized via CO_2 asphyxiation and the intradermal sites of injection were lavaged with two 1-ml quantities of sterile 0.7% saline. The lavage fluid was adjusted to a fixed volume and bacterial survival was estimated via serial dilution of the lavage fluid, plating out and enumeration of the recovered bacteria after overnight incubation. Survival was expressed as: recovered GAS CFU/CFU of inoculum*100%. Remaining lavage fluid was washed once with sterile PBS and labelled with rat anti-mouse Ly6-G phycoerythrin-conjugated IgG (clone: 1A8, Biolegend) and GAS association with murine PMNs was assessed as described for purified human PMNs. For animal studies involving histological staining, including by TUNEL, C57BL/6J mice were infected with 5×10^7 CFU of mid-logarithmic phase, non-eGFP-expressing GAS and euthanized by CO_2 24 h after infection. Infected murine dermal tissue was then harvested, formalin-fixed and paraffin-embedded prior to microtome sectioning and hematoxylin and eosin (HE) staining, using standard protocols. Identification of apoptotic cells was conducted using the DEADend fluorometric TUNEL kit (Promega) instructions for paraffin-embedded tissues. TUNEL-stained tissues were analyzed using a Leica TCS SP5 laser scanning confocal microscope (Leica, Wetzlar, Germany). For animal cytokine studies, C57BL/6J mice were subcutaneously infected with 1×10^7 CFU for 48 h. Blood was harvested from the apex of the heart and serum was collected and stored at –20°C until use. Murine TNF-α, IL-6 and IL-1β levels were quantified in duplicate by ELISA as per the manufacturer's instructions (Biolegend).

Cytotoxicity

GAS-induced PMN cytotoxicity was assessed essentially as previously [6]. Briefly, 2×10^5 human PMNs were infected with 2×10^6 GAS CFU and incubated for varying periods of time, 50-μl aliquots of cell supernatants were then sampled and the lactate *D*-dehydrogenase (LDH) concentration was measured using the CytoTox 96 kit (Promega) according to the manufacturer's instructions. Cytotoxicity was calculated as LDH release induced by either GAS strain over maximum LDH release (total LDH from lysed uninfected cells) corrected for the spontaneous release of LDH from uninfected cells. For some experiments, PMNs were infected in the presence of 100 mM of glycine.

Electron Microscopy

For scanning electron microscopy, 5×10^6 PMNs were infected with 5×10^7 GAS CFU for 5 h. Samples were fixed with 5% formaldehyde and 2% glutaraldehyde in HEPES buffer, and kept at 4°C before dehydrating with a graded series of acetone, critical-point-dried with CO_2 and sputter-coated with gold-palladium. Samples were examined under a Zeiss Merlin microscope (Carl Zeiss) at an acceleration voltage of 5 kV using the Everhart-Thornley SE-detector and the Inlens SE-detector in a 25:75 ratio. For transmission electron microscopy, PMNs were infected and samples fixed as above, and treated with 1% aqueous osmium tetroxide for 1 h prior to dehydration with a graded series of acetone, treatment with 2% uranyl acetate in 70% acetone for overnight, further dehydration with acetone, and embedding in Spurr epoxide resin. Ultrathin sections were cut with a diamond knife, counterstained with uranyl acetate and observed under a Zeiss EM910 microscope at an acceleration voltage of 80 kV. Images were recorded digitally with a slow-scan CCD camera (ProScan, 1024 × 1024) with ITEM-Software (Olympus, Tokyo, Japan). Contrast and brightness of images were adjusted with Adobe Photoshop (Adobe Systems, San Jose, USA).

Statistical Analyses

Statistical analysis of differences between conditions for PMN phagocytosis, LDH release, bacterial survival in vivo and systemic cytokine assays were conducted using the unpaired Student t test. Differences between conditions for TUNEL, Ψ_m depolarization and osmoprotection assays were analyzed using one-way ANOVA with the Tukey multiple-comparison test. Differences in survival curves were analyzed using a log-rank (Mantel-Cox) test. Differences were deemed statistically significant at $p < 0.05$. All statistical analyses were conducted using Prism 5 (GraphPad Software Inc., La Jolla, Calif., USA).

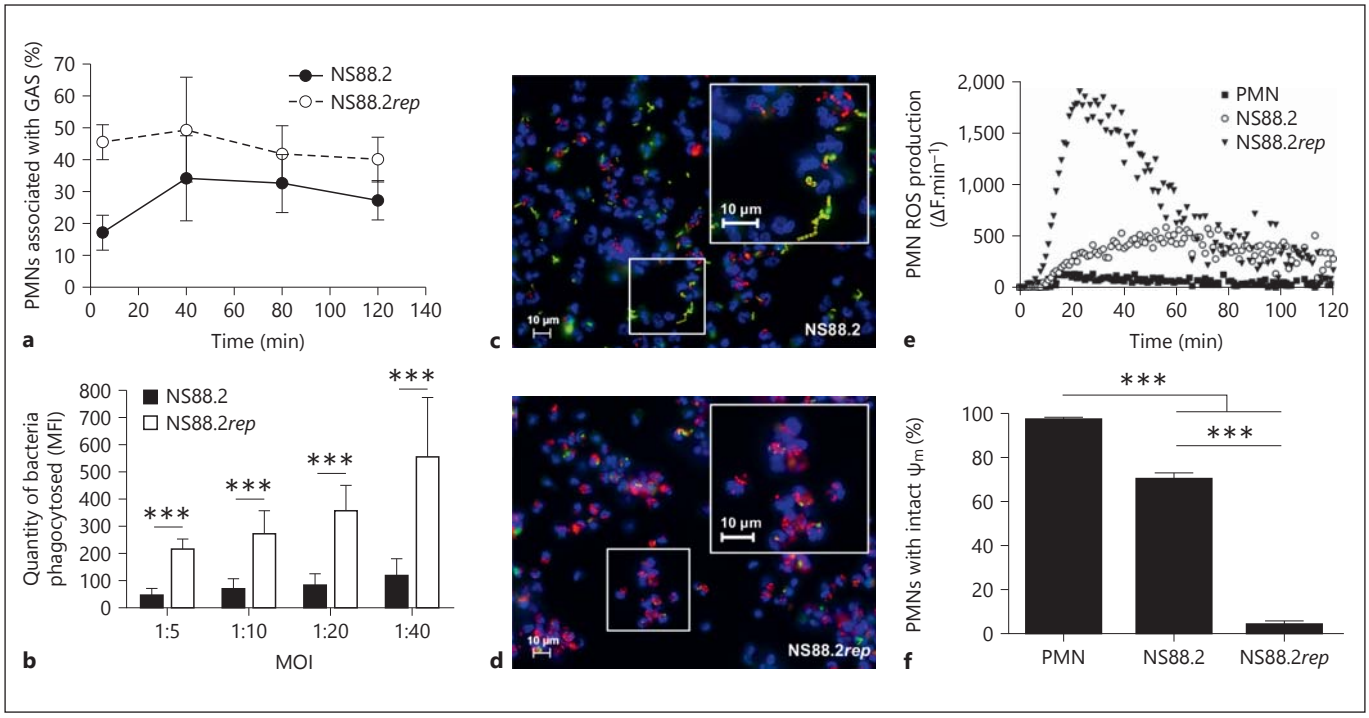

Fig. 1. PMN phagocytosis, ROS production and mitochondrial membrane depolarization are differentially modulated by virulent GAS. **a** PMN phagocytosis of virulent GAS strain NS88.2 and avirulent GAS strain NS88.2*rep* at a constant MOI of 10:1. **b** Relative quantification of NS88.2 and NS88.2*rep* phagocytosis at increasing MOIs. **c**, **d** Double immunofluorescence microscopy of PMNs infected for 30 min with NS88.2 (**c**) or NS88.2*rep* (**d**). Inset: shows a higher magnification. Extracellular GAS (yellow); intracellular GAS (red); PMN nuclei (blue). **e** GAS-induced PMN ROS production during NS88.2 or NS88.2*rep* infection. ROS production is expressed as a change in relative fluorescence units over time ($\Delta F.min^{-1}$). **f** Determination of the ψ_m of GAS-infected PMNs. Microscope images were altered for brightness to highlight infecting GAS cells. **a**, **b**, **f** Results are pooled means ± SD (n = 3). **e** Results are pooled means (n = 4). **c**, **d** Images are representative of duplicate experiments. *** $p < 0.001$.

Results

PMN Phagocytosis, ROS Production and Mitochondrial Membrane Depolarization Are Differentially Modulated by Virulent GAS

The initial interactions of PMNs with GAS are mediated via phagocytosis of the infecting bacteria. Incubation of eGFP-expressing virulent GAS (NS88.2) and avirulent GAS (NS88.2*rep*) with PMNs revealed that phagocytosis occurred rapidly for both NS88.2 and NS88.2*rep* GAS (<5 min), with a higher percentage of PMNs tending to associate with NS88.2*rep* compared with NS88.2 (fig. 1a). The relative quantity of NS88.2*rep* associated with each PMN cell was significantly higher than NS88.2, an effect that was exaggerated at increasing MOIs (fig. 1b, $p < 0.001$ for all). NS88.2 was frequently visualized in the extracellular space during PMN infection, whereas NS88.2*rep* was more often localized within infected PMNs (fig. 1c, d). This difference in phagocytosis was not due to differences in growth kinetics, as both strains showed equal growth rates in THY media alone (online suppl. fig. S2).

The PMN respiratory burst against ingested pathogens plays a key role in the destruction of phagocytosed microbes and in the regulation of downstream cell death pathways. Kinetic measurement of PMN ROS production during phagocytosis of GAS revealed that avirulent NS88.2*rep* GAS stimulated higher ROS activity than the virulent NS88.2 strain (fig. 1e). ROS also play an important function in the regulation of the Ψ_m, which, in turn, reflects cellular viability, as uncoupling of this proton gradient plays a central role in multiple cell death pathways [17]. Incubation with NS88.2*rep* elicited a large, significant reduction in Ψ_m compared with uninfected PMNs and cells infected with NS88.2 ($p < 0.001$; fig. 1f). Infection of PMNs with NS88.2 also elicited a significant, albeit smaller reduction in Ψ_m compared to uninfected cells ($p < 0.001$; fig. 1f). Collectively, these results suggest that

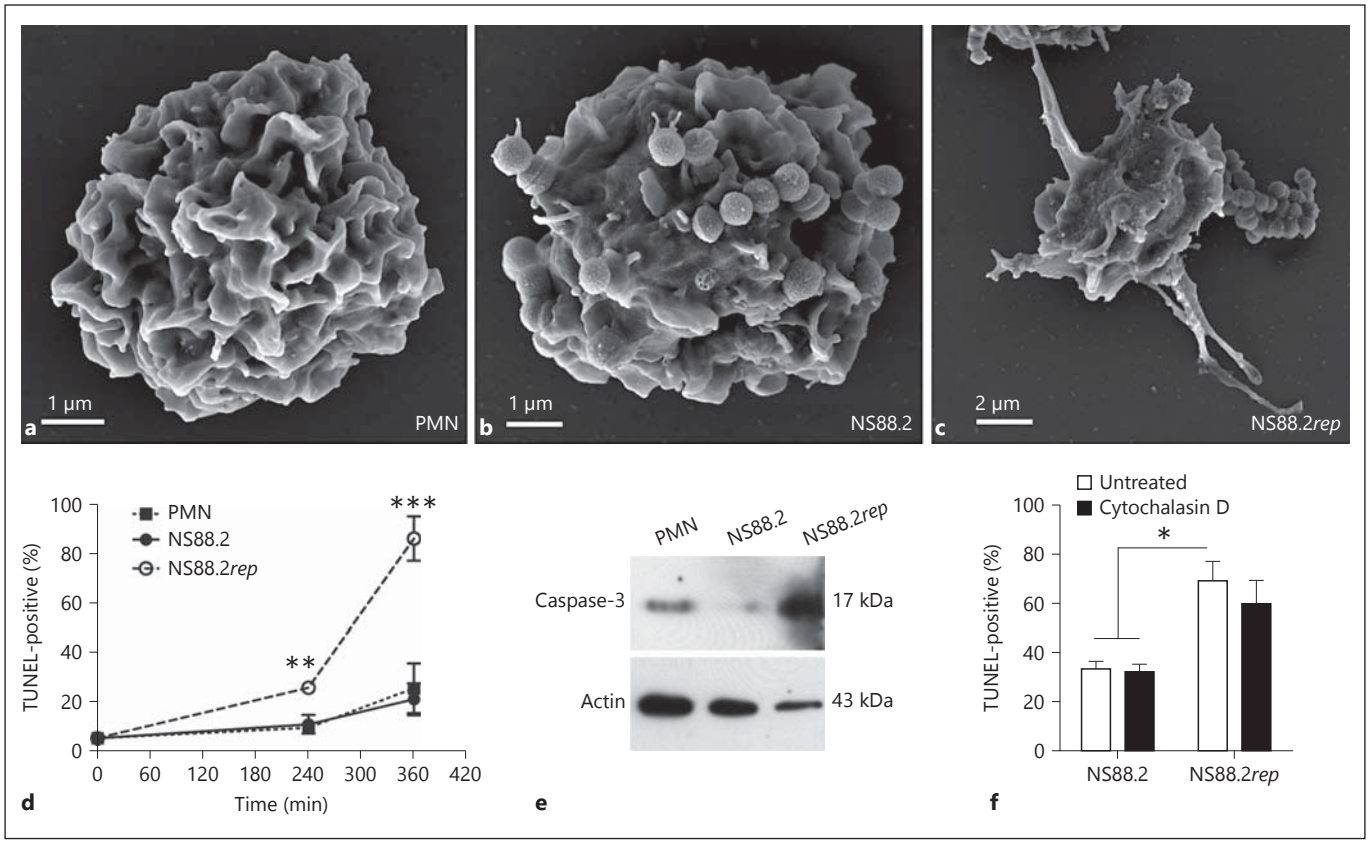

Fig. 2. Avirulent GAS promotes PMN apoptotic responses. Uninfected PMNs (**a**), PMNs infected with NS88.2 (**b**) or with NS88.2*rep* (**c**) were analyzed by scanning electron microscopy 5 h after infection. **d** Quantification of oligonucleosomal DNA fragmentation of uninfected PMNs and PMNs infected with NS88.2 and NS88.2*rep* by TUNEL. **e** Detection of active caspase-3 protein in uninfected PMNs, NS88.2-infected and NS88.2*rep*-infected PMNs by Western blot 5 h after infection. **f** TUNEL staining of Cytochalasin D (5 µg/ml)-treated PMNs infected for 6 h with NS88.2 and NS88.2*rep*. **d**, **f** Results are pooled means ± SD (n = 3). **e** Results are representative of duplicate experiments. * $p < 0.05$; ** $p < 0.01$; *** $p < 0.001$.

downstream PMN cell death responses, such as apoptosis, may be influenced by differential ROS generation and Ψ_m depolarization after the phagocytosis of GAS.

Avirulent GAS Infection Induces an Apoptotic PMN Phenotype

With many forms of cell death pathways, cells undergo characteristic alterations in external morphology that are indicative of cell death mechanisms [18]. Visualization of GAS-induced PMN cell death was conducted by scanning electron microscopy 5 h after infection. Uninfected PMNs exhibited typical neutrophil exterior morphology with few membrane irregularities (fig. 2a). Comparatively, NS88.2-infected PMNs exhibited slight cellular swelling but membrane morphology similar to the uninfected cells (fig. 2b). In contrast, NS88.2*rep*-infected PMNs exhibited both cellular shrinkage and extensive membrane blebbing, both features indicative of apoptotic cell death (fig. 2c).

Biochemical interrogation of GAS-induced cell death was conducted via fluorescent measurement of nuclear DNA fragmentation (TUNEL staining) and caspase-3 cleavage. Infection of human PMNs with the avirulent NS88.2*rep* strain induced significantly higher TUNEL staining at 4 h ($p < 0.01$) and 6 h ($p < 0.001$) after infection compared to both NS88.2-infected and uninfected PMNs (fig. 2d), whereas NS88.2 infection induced comparable TUNEL staining to uninfected cells ($p > 0.05$). An increased amount of the active caspase-3 protein was present in NS88.2*rep*-infected cells relative to uninfected and NS88.2-infected cells 5 h after infection (fig. 2e), further indicating an apoptotic cellular response in the PMNs exposed to NS88.2*rep*. To determine whether PMN apoptotic responses were phagocytosis-dependent,

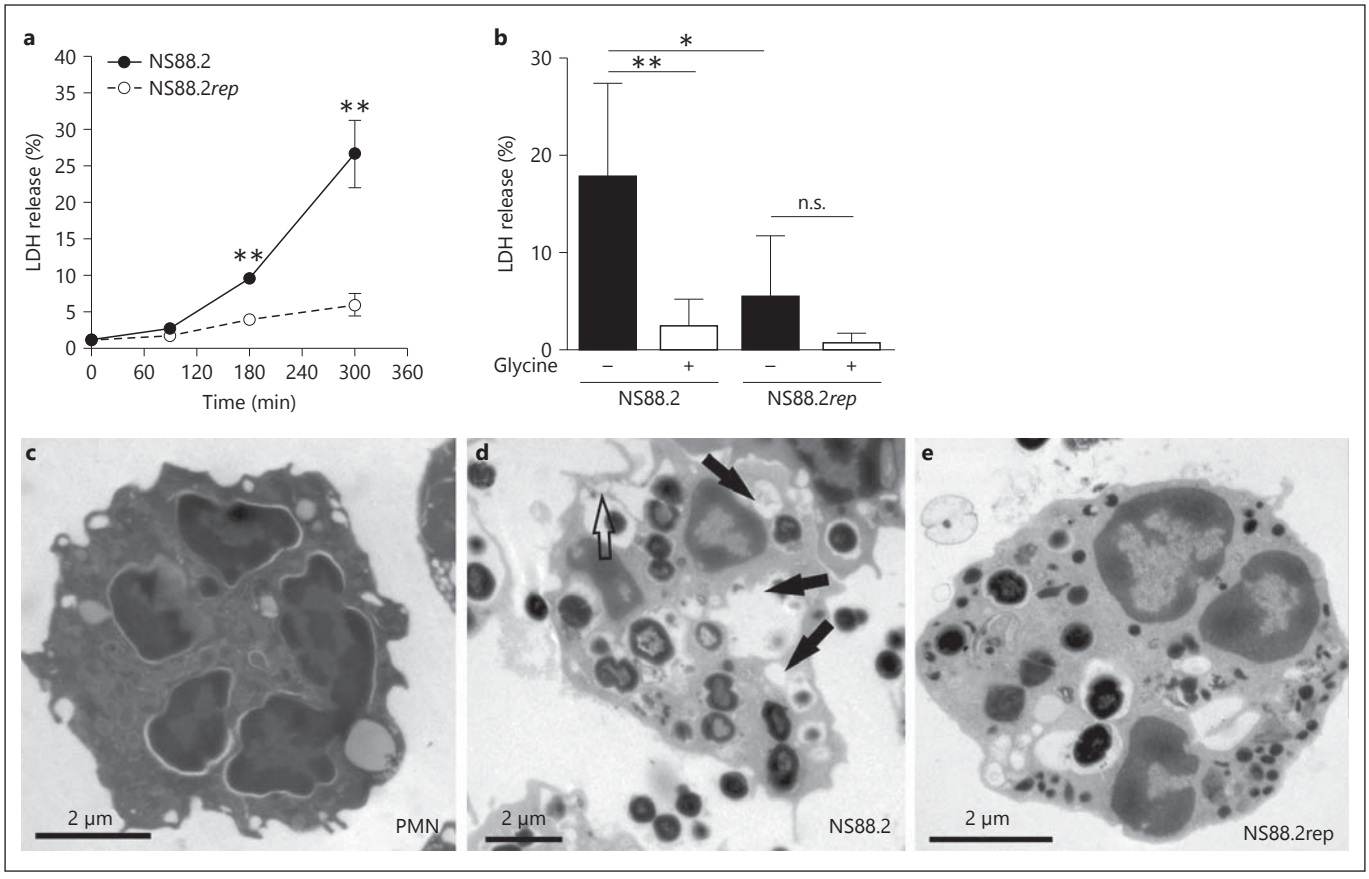

Fig. 3. PMN cell death induced by virulent GAS is associated with loss of membrane integrity and vacuolization. **a** Quantification of NS88.2-induced and NS88.2*rep*-induced PMN plasma membrane permeabilization via LDH measurement over time. **b** Quantification of LDH released in response to NS88.2 and NS88.2*rep* infection in the presence of glycine 6 h after infection. Transmission electron microscopy of uninfected (**c**), NS88.2-infected (**d**) and NS88.2*rep*-infected (**e**) human PMNs 5 h after infection. Filled arrowheads indicate PMN vacuoles and unfilled arrowheads indicate cell membrane disruption. **a** Results are representative of means ± SD of 1 experiment (n = 4). **b** Results are pooled means ± SD (n = 2). n.s. = Not significant. * $p < 0.05$; ** $p < 0.01$.

PMNs were preincubated with the actin polymerization inhibitor cytochalasin D prior to infection to prevent GAS uptake. No significant difference in TUNEL staining was noted for PMNs treated with cytochalasin D relative to untreated PMNs for either the avirulent NS88.2*rep* or virulent NS88.2 strains (fig. 2f).

PMNs Infected by Virulent GAS Exhibit Plasma Membrane Disintegration and a Necrotic Cell Death Modality

Orchestrated necrotic leukocyte mechanisms (also referred to as oncosis) have been previously shown to result in proinflammatory phenotypes, and they precede cell death following infection by other pathogens [19, 20]. To investigate the potential necrotic consequences of GAS infection of PMNs, cell membrane integrity (LDH release) was assayed (fig. 3a). Infection of PMNs with NS88.2*rep* resulted in minimal LDH release and maintenance of plasma membrane impermeability, in contrast to NS88.2-infected PMNs which provoked significantly higher LDH release ($p < 0.05$). Higher rates of LDH release in response to infection by NS88.2 but not NS88.2*rep* could be significantly reduced through the addition of the osmoprotectant glycine (fig. 3b). Substantiating this biochemical data, transmission electron microscopy revealed a large degree of vacuolization and evidence of cell membrane disintegration in NS88.2-infected PMNs in comparison to NS88.2*rep*-infected and uninfected cells 5 h after infection (fig. 3c–e). Both extensive vacuolization and loss of cell membrane integrity have been previously associated with necrotic cell death processes, leading to proinflammatory cell responses [21]. Although

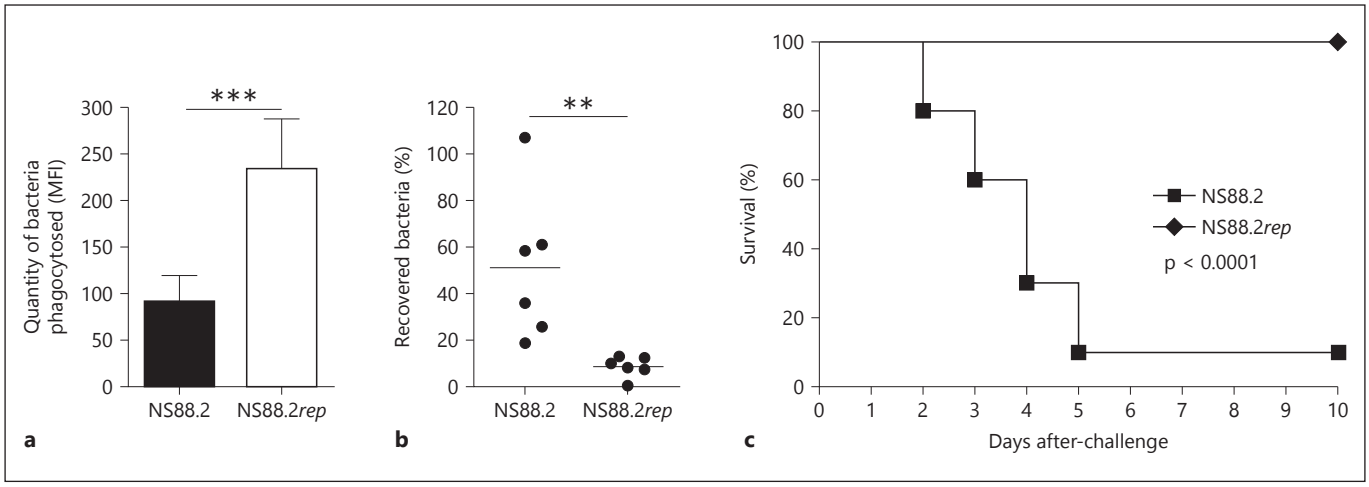

Fig. 4. Murine PMN phagocytosis and killing of virulent GAS is impaired in vivo, leading to mortality. **a** Relative quantification of NS88.2 and NS88.2*rep* phagocytosis by murine Ly6-G$^+$ neutrophils. **b** NS88.2 and NS88.2*rep* cutaneous survival in vivo. Survival is expressed as percentage recovered bacteria over inoculum. **c** Survival of wild-type C57BL/6J mice subcutaneously infected with 9×10^7 CFU of NS88.2 or NS88.2*rep*. **a**, **b** Results are pooled means ± SD (n = 3). ** $p < 0.01$; *** $p < 0.001$.

proinflammatory PMN cell death responses are well-characterized in vitro, the in vivo role of GAS-induced necrotic PMN cell death and necrotic PMN-mediated inflammatory responses is not so well-defined.

PMNs Recruited to Virulent GAS Infection Have Impaired Apoptotic Ability and Accompany Heightened Inflammatory Responses

Necrotic PMN cell death results in eventual cell lysis and, as such, the release of damage-associated molecular pattern molecules (DAMPs) from these injured and dying cells [8]. GAS-induced dysregulation from a more physiological apoptotic PMN response may contribute to the destructive tissue pathologies noted in murine infection models, and in clinical manifestations of severe GAS disease [22]. To characterize the dynamics of PMNs recruited to virulent GAS infection in vivo, C57BL/6J mice were intradermally injected with eGFP-expressing NS88.2 and NS88.2*rep*, and the infection site was lavaged 6 h after infection. Murine neutrophils (Ly6-G$^+$ cells) showed an increased uptake of NS88.2*rep* compared with NS88.2 (fig. 4a, $p < 0.001$), corroborating previous data described above using human PMNs. Reduced phagocytic uptake of NS88.2 by murine neutrophils is likely to contribute to the significantly enhanced survival of this strain within the dermis of infected mice at 6 h (fig. 4b, $p < 0.01$) and to NS88.2 virulence during 10-day infection, relative to NS88.2*rep* (fig. 4c, $p < 0.001$).

Histopathological assessment of HE-stained infected murine dermal tissues was undertaken 24 h after infection. Saline injection did not engender any adverse histopathologies (fig. 5a–c). Infection with virulent NS88.2 elicited suppurative inflammation manifested by robust PMN infiltration (fig. 5d, e, filled arrowheads). Infiltrating PMNs exhibited a high degree of pyknotic (fig. 5f, filled arrowheads) and karyorrhexic (fig. 5f, unfilled arrowheads) nuclei morphologies. Intradermal infection with avirulent NS88.2*rep* also elicited PMN infiltration (fig. 5g). Infiltrates to the site of NS88.2*rep* infection were primarily PMNs (fig. 5h, filled arrowheads), and displayed frequent pyknotic cell morphology (fig. 5i, filled arrowheads) with the appearance of numerous apoptotic body structures (fig. 5i, unfilled arrowheads). Systemic levels of several classic proinflammatory cytokines were also assessed 48 h after GAS infection (fig. 6a–c). The circulating levels of TNF-α and IL-6 were significantly higher in mice infected with NS88.2 than with NS88.2*rep* (fig. 6a, b, $p < 0.05$). Circulating levels of IL-1β were also increased in NS88.2-infected mice, though this difference was not statistically significant (fig. 6c, $p > 0.05$).

Biochemical analysis of murine infiltrates associated with GAS infection was assessed via TUNEL to confirm apoptotic nuclear DNA fragmentation (fig. 7a–i). Saline injection was not associated with significant TUNEL staining (fig. 7a–c). Cells associated with NS88.2 infection were infrequently TUNEL-positive, indicating a paucity of apoptotic cell nuclei (fig. 7d–f). Infiltrating cells within and surrounding the bolus of NS88.2*rep* infection exhibited stronger and more frequent positive TUNEL staining

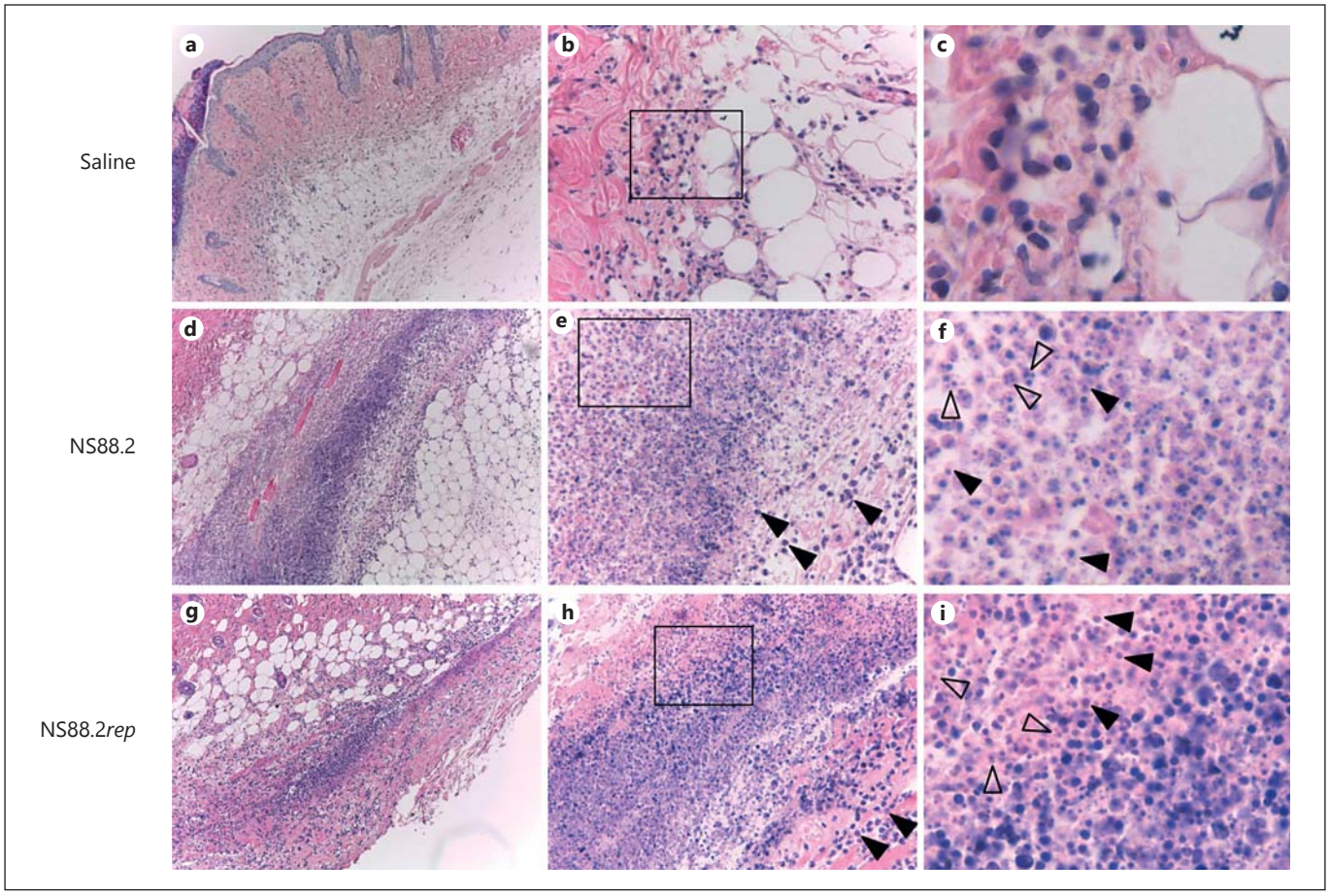

Fig. 5. Murine PMNs exhibit degeneracy and adverse histopathologies during cutaneous infection by virulent GAS. Murine dermis injected with sterile saline (**a–c**), NS88.2 (**d–f**) or NS88.2*rep* (**g–i**) was HE-stained 24 h after injection. **e**, **h** PMNs (filled arrowheads). **f**, **i** Pyknotic cells (filled arrowheads). **f** Karyorrhexic cells (unfilled arrowheads). **i** Apoptotic bodies (unfilled arrowheads). **a**, **d**, **g** ×10. **b**, **e**, **h** ×40. **c**, **f**, **i** ×460.

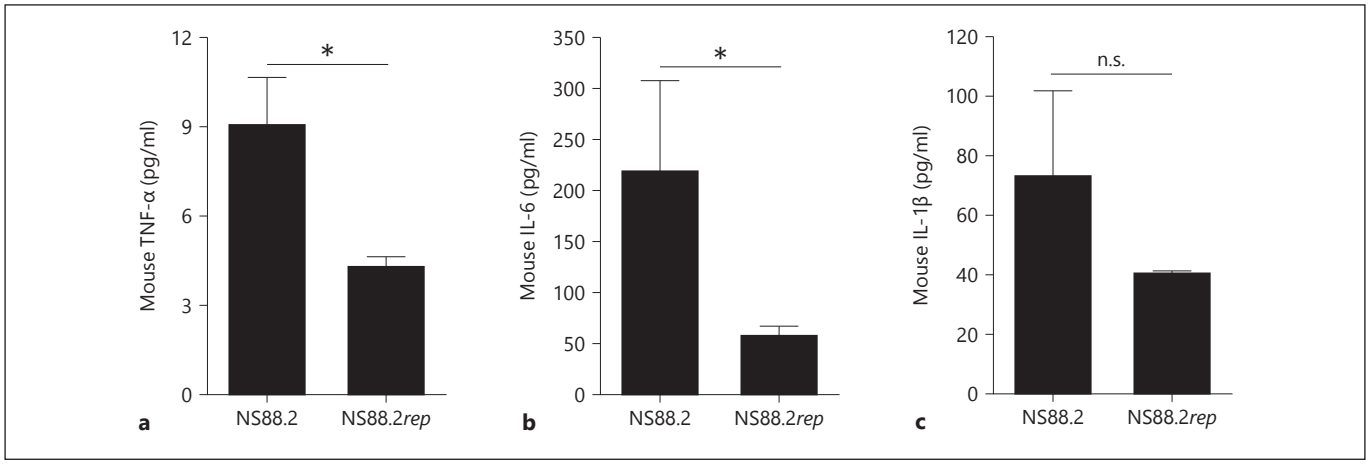

Fig. 6. Systemic proinflammatory cytokines are increased in virulent GAS infection. C57BL/6J mice were subcutaneously infected with NS88.2 or NS88.2*rep* for 48 h and the circulating levels of TNF-α (**a**), IL-6 (**b**) and IL-1β (**c**) quantified by ELISA. **a**, **c** Results are pooled means ± SD (n = 3). n.s. = Not significant. * $p < 0.05$.

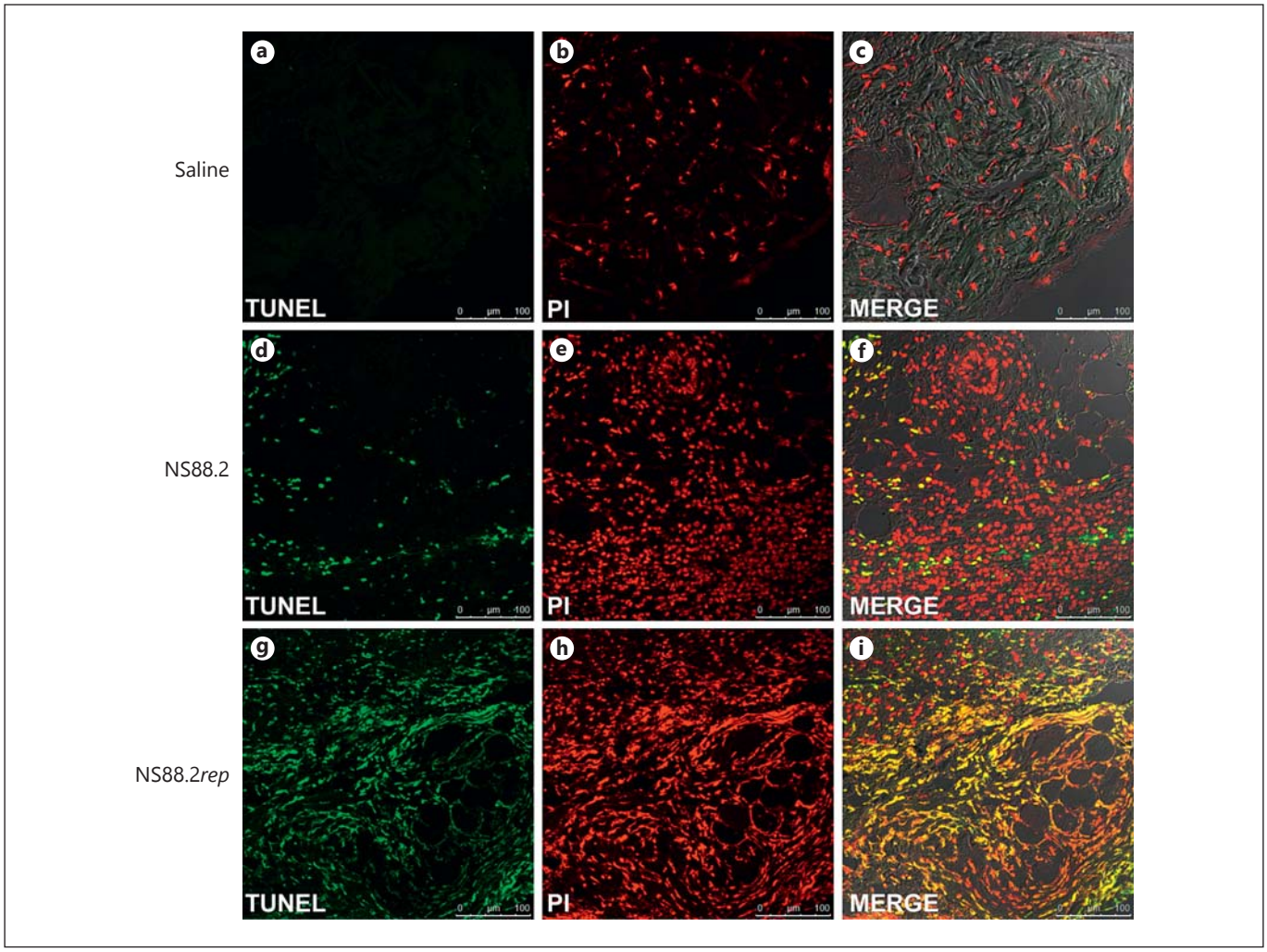

Fig. 7. Dermal cells responding to cutaneous infection by virulent GAS infection exhibit decreased apoptosis. Murine dermis injected with sterile saline (**a–c**), NS88.2 (**d–f**) or NS88.2*rep* (**g–i**) was stained 24 h after injection using TUNEL to detect apoptotic cells (**a**, **d**, **g**); propidium iodide (PI) as a counterstain for the total cell population (**b**, **e**, **h**) and merged channels with differential interference (**c**, **f**, **i**). Results shown are representative of quadruplicate sections taken from 6 flanks of 3 animals per condition.

(fig. 7g–i). Thus, immunohistological evidence supports the in vitro data described above, and demonstrates that PMNs recruited to cutaneous, virulent GAS infection display a reduced apoptotic phenotype.

Discussion

Induction of PMN apoptosis is critical for the resolution of inflammation in a variety of noninfectious and infectious scenarios, including wound-healing, meningitis and pneumonia [23]. This process is essential for preventing excessive inflammatory reactions, whereby aging cells and cells recruited to sites of infection may be disposed of safely without the sustained stimulation of immune responses. In animal models of meningitis, the persistence of PMNs lacking crucial apoptotic factors is strongly associated with adverse clinical outcomes [24]. Our study indicates that interaction with avirulent GAS elicits a programmed PMN cell death mechanism that is apoptotic in nature. Avirulent GAS elicits robust PMN ROS production, triggering downstream mitochondrial membrane depolarization and activation of the primary apoptotic effector, caspase-3. Despite higher rates of phagocytosis of avirulent GAS by both murine and human PMNs, the inhibition of human PMN phagocytosis

did not reduce TUNEL staining of human PMNs (fig. 2f). This suggests that avirulent GAS may induce human PMN apoptosis via secreted products, as has been described for the interaction of GAS cysteine protease SpeB with epithelial cells [25].

These data indicate that exposure to avirulent GAS elicits a regulated PMN cell death mechanism reflective of the caspase-dependent, intrinsic apoptotic pathway [26]. The induction of apoptotic PMN cell death by avirulent GAS could be crucial for preventing excessive inflammatory reactions, whereby PMNs exhausted from microbicidal responsibilities may be disposed of safely, without undue immune stimulation [23]. As apoptotic cell death does not induce further inflammatory responses, it is considered to be immunologically silent [27]. However, exposure to virulent GAS appears to elicit a distinct PMN cell death process that lacks typical apoptotic markers.

Rigorous biochemical identification of oncosis is problematic, given that few broadly applicable markers have been identified [18]. In this regard, we did not observe the rapid ATP depletion or ionic disturbances in response to virulent GAS infection, as has been noted in previous accounts of cellular oncosis (data not shown) [21, 28]. Recent guidelines governing the molecular definitions of cell death mechanisms recommend the use of general, as opposed to specific, nomenclature regarding cell death programs [17]. As such, we report that virulent GAS induce a proinflammatory form of cell death in PMNs which lacks common apoptotic markers and shares many of those reported for regulated necrosis.

Necrotic leukocyte cell death responses have been previously shown to result in a proinflammatory phenotype, and they precede leukocyte cell death following infection by other pathogens [19, 20]. However, there is still a dearth of literature concerning the mechanisms by which these processes proceed in PMNs, the relationship between infection-mediated PMN cell death responses and inflammation during disease. Here, we show that, in contrast to avirulent GAS, PMNs infected with virulent GAS undergo mitochondrial membrane depolarization, as shown for avirulent GAS, but this event precedes the early loss of plasma membrane integrity and vacuolization. In vivo data describing the pathophysiological relevance of leukocyte cell death has been lacking. We propose that the manner of PMN cell death by either apoptosis or more necrotic forms affects the magnitude and nature of subsequent host immune responses.

Multiple reports have described a pivotal role for pore-forming toxins in other bacteria in shaping host leukocyte responses, including the GAS cytotoxins SLO and SLS [29, 30]. Virulent GAS bestowed with *covRS* mutations are highly encapsulated, and express higher levels of SLO, so PMN necrosis is likely due in part to cytolysin-expressing extracellular GAS. Induction of PMN apoptosis has been postulated as a viable strategy to reduce harmful pathologies during acute inflammation [23, 31]. In support of this proposition, there are studies showing treatment of mice with cyclin-dependent kinase inhibitors that induce PMN apoptosis and improve the resolution of inflammation and clinical symptoms during experimental pneumococcal infection [32, 33]. Cyclin-dependent kinase inhibitors show promise as novel anti-inflammatory therapeutics [34].

In summary, this work describes dynamic host PMN cell death responses to GAS infection. PMN cell death in response to avirulent GAS infection is associated with an apoptotic program whereas PMNs recruited to virulent GAS infection in the dermis lack apoptotic markers and bear hallmarks of proinflammatory cell death, which may amplify immune reactions during infection.

Acknowledgements

We thank I. Schleicher for help with electron microscopic analyses. This work was supported by the National Health and Medical Research Council of Australia (grant numbers 635218 and 1009369 to M.L.S.-S.).

Disclosure Statement

The authors have no conflicts of interest to declare.

References

1 Kennedy AD, DeLeo FR: Neutrophil apoptosis and the resolution of infection. Immunol Res 2009;43:25–61.

2 Kobayashi SD, Braughton KR, Whitney AR, Voyich JM, Schwan TG, Musser JM, DeLeo FR: Bacterial pathogens modulate an apoptosis differentiation program in human neutrophils. Proc Natl Acad Sci U S A 2003;100:10948–10953.

3 Kobayashi SD, Voyich JM, Braughton KR, DeLeo FR: Down-regulation of proinflammatory capacity during apoptosis in human polymorphonuclear leukocytes. J Immunol 2003;170:3357–3368.

4 Silva MT: Macrophage phagocytosis of neutrophils at inflammatory/infectious foci: a cooperative mechanism in the control of infection and infectious inflammation. J Leukoc Biol 2011;89:675–683.

5 Bratton DL, Henson PM: Neutrophil clearance: when the party is over, clean-up begins. Trends Immunol 2011;32:350–357.
6 Goldmann O, Sastalla I, Wos-Oxley M, Rohde M, Medina E: *Streptococcus pyogenes* induces oncosis in macrophages through the activation of an inflammatory programmed cell death pathway. Cell Microbiol 2009;11:138–155.
7 Fink SL, Cookson BT: Pyroptosis and host cell death responses during *Salmonella* infection. Cell Microbiol 2007;9:2562–2570.
8 Kono H, Rock KL: How dying cells alert the immune system to danger. Nat Rev Immunol 2008;8:279–289.
9 Walker MJ, Barnett TC, McArthur JD, Cole JN, Gillen CM, Henningham A, Sriprakash KS, Sanderson-Smith ML, Nizet V: Disease manifestations and pathogenic mechanisms of group A *Streptococcus*. Clin Microbiol Rev 2014;27:264–301.
10 Cole JN, Barnett TC, Nizet V, Walker MJ: Molecular insight into invasive group A streptococcal disease. Nat Rev Microbiol 2011;9:724–736.
11 Carapetis JR, Steer AC, Mulholland EK, Weber M: The global burden of group A streptococcal diseases. Lancet Infect Dis 2005;5:685–694.
12 Lamagni TL, Darenberg J, Luca-Harari B, Siljander T, Efstratiou A, Henriques-Normark B, Vuopio-Varkila J, Bouvet A, Creti R, Ekelund K, Koliou M, Reinert RR, Stathi A, Strakova L, Ungureanu V, Schalen C, Jasir A, Grp S-ES: Epidemiology of severe *Streptococcus pyogenes* disease in Europe. J Clin Microbiol 2008;46:2359–2367.
13 Norrby-Teglund A, Chatellier S, Low DE, McGeer A, Green K, Kotb M: Host variation in cytokine responses to superantigens determines the severity of invasive group A streptococcal infection. Eur J Immunol 2000;30:3247–3255.
14 Maamary PG, Sanderson-Smith ML, Aziz RK, Hollands A, Cole JN, McKay FC, McArthur JD, Kirk JK, Cork AJ, Keefe RJ, Kansal RG, Sun H, Taylor WL, Chhatwal GS, Ginsburg D, Nizet V, Kotb M, Walker MJ: Parameters governing invasive disease propensity of non-M1 serotype group A streptococci. J Innate Immun 2010;2:596–606.
15 Jeng A, Sakota V, Li Z, Datta V, Beall B, Nizet V: Molecular genetic analysis of a group A *Streptococcus* operon encoding serum opacity factor and a novel fibronectin-binding protein, SfbX. J Bacteriol 2003;185:1208–1217.
16 Ly D, Taylor JM, Tsatsaronis JA, Monteleone MM, Skora AS, Donald CA, Maddocks T, Nizet V, West NP, Ranson M, Walker MJ, McArthur JD, Sanderson-Smith ML: Plasmin(ogen) acquisition by group A *Streptococcus* protects against C3b-mediated neutrophil killing. J Innate Immun 2014;6:240–250.
17 Galluzzi L, Vitale I, Abrams JM, Alnemri ES, Baehrecke EH, Blagosklonny MV, Dawson TM, Dawson VL, El-Deiry WS, Fulda S, Gottlieb E, Green DR, Hengartner MO, Kepp O, Knight RA, Kumar S, Lipton SA, Lu X, Madeo F, Malorni W, Mehlen P, Nunez G, Peter ME, Piacentini M, Rubinsztein DC, Shi Y, Simon HU, Vandenabeele P, White E, Yuan J, Zhivotovsky B, Melino G, Kroemer G: Molecular definitions of cell death subroutines: recommendations of the Nomenclature Committee on Cell Death 2012. Cell Death Diff 2012;19:107–120.
18 Kroemer G, Galluzzi L, Vandenabeele P, Abrams J, Alnemri ES, Baehrecke EH, Blagosklonny MV, El-Deiry WS, Golstein P, Green DR, Hengartner M, Knight RA, Kumar S, Lipton SA, Malorni W, Nunez G, Peter ME, Tschopp J, Yuan J, Piacentini M, Zhivotovsky B, Melino G: Classification of cell death: Recommendations of the Nomenclature Committee on Cell Death 2009. Cell Death Diff 2009;16:3–11.
19 Dacheux D, Toussaint B, Richard M, Brochier G, Croize J, Attree I: *Pseudomonas aeruginosa* cystic fibrosis isolates induce rapid, type III secretion-dependent but ExoU-independent, oncosis of macrophages and polymorphonuclear neutrophils. Infect Immun 2000;68:2916–2924.
20 Bergsbaken T, Cookson BT: Innate immune response during *Yersinia* infection: critical modulation of cell death mechanisms through phagocyte activation. J Leukoc Biol 2009;86:1153–1158.
21 Fink SL, Cookson BT: Apoptosis, pyroptosis, and necrosis: mechanistic description of dead and dying eukaryotic cells. Infect Immun 2005;73:1907–1916.
22 Stevens DL, Bisno AL, Chambers HF, Everett ED, Dellinger P, Goldstein EJ, Gorbach SL, Hirschmann JV, Kaplan EL, Montoya JG, Wade JC; Infectious Diseases Society of America: Practice guidelines for the diagnosis and management of skin and soft-tissue infections. Clin Infect Dis 2005;41:1373–1406.
23 Fox S, Leitch AE, Duffin R, Haslett C, Rossi AG: Neutrophil apoptosis: relevance to the innate immune response and inflammatory disease. J Innate Immun 2010;2:216–227.
24 Garrison SP, Thornton JA, Hacker H, Webby R, Rehg JE, Parganas E, Zambetti GP, Tuomanen EI: The p53-target gene puma drives neutrophil-mediated protection against lethal bacterial sepsis. PLoS Pathog 2010;6:e1001240.
25 Tsai P-J, Lin Y-S, Kuo C-F, Lei H-Y, Wu J-J: Group A *Streptococcus* induces apoptosis in human epithelial cells. Infect Immun 1999;67:4334–4339.
26 Elmore S: Apoptosis: a review of programmed cell death. Toxicol Pathol 2007;35:495–516.
27 Labbe K, Saleh M: Cell death in the host response to infection. Cell Death Diff 2008;15:1339–1349.
28 Trump BE, Berezesky IK, Chang SH, Phelps PC: The pathways of cell death: oncosis, apoptosis, and necrosis. Toxicol Pathol 1999;25:82–88.
29 Miyoshi-Akiyama T, Takamatsu D, Koyanagi M, Zhao J, Imanishi K, Uchiyama T: Cytocidal effect of *Streptococcus pyogenes* on mouse neutrophils in vivo and the critical role of streptolysin S. J Infect Dis 2005;192:107–116.
30 Tsatsaronis JA, Walker MJ, Sanderson-Smith ML: Host responses to group A *Streptococcus*: cell death and inflammation. PLoS Pathog 2014;10:e1004266.
31 Rossi AG, Sawatzky DA, Walker A, Ward C, Sheldrake TA, Riley NA, Caldicott A, Martinez-Losa M, Walker TR, Duffin R, Gray M, Crescenzi E, Martin MC, Brady HJ, Savill JS, Dransfield I, Haslett C: Cyclin-dependent kinase inhibitors enhance the resolution of inflammation by promoting inflammatory cell apoptosis. Nat Med 2006;12:1056–1064.
32 Koedel U, Frankenberg T, Kirschnek S, Obermaier B, Hacker H, Paul R, Hacker G: Apoptosis is essential for neutrophil functional shutdown and determines tissue damage in experimental pneumococcal meningitis. PLoS Pathog 2009;5:e1000461.
33 Hoogendijk AJ, Roelofs JJ, Duitman J, van Lieshout MH, Blok DC, van der Poll T, Wieland CW: R-roscovitine reduces lung inflammation induced by lipoteichoic acid and *Streptococcus pneumoniae*. Mol Med 2012;18:1086–1095.
34 Leitch AE, Haslett C, Rossi AG: Cyclin-dependent kinase inhibitor drugs as potential novel anti-inflammatory and pro-resolution agents. Br J Pharmacol 2009;158:1004–1016.